radiation

MDPI

Review

Investigation on Rare Nuclear Processes in Hf Nuclides

Vincenzo Caracciolo [1,2,*], Pierluigi Belli [1,2], Rita Bernabei [1,2], Fabio Cappella [3,4], Riccardo Cerulli [1,2], Antonella Incicchitti [3,4], Matthias Laubenstein [5], Alice Leoncini [1,2], Vittorio Merlo [1,2], Serge Nagorny [6,7], Stefano Nisi [5] and Peng Wang [6,8]

1 Dipartimento di Fisica, Università di Roma "Tor Vergata", 00133 Rome, Italy; pierluigi.belli@roma2.infn.it (P.B.); rita.bernabei@roma2.infn.it (R.B.); riccardo.cerulli@roma2.infn.it (R.C.); alice.leoncini@roma2.infn.it (A.L.); vittorio.merlo@roma2.infn.it (V.M.)
2 INFN, Sezione di Roma "Tor Vergata", 00133 Rome, Italy
3 INFN, Sezione Roma "La Sapienza", 00185 Rome, Italy; fabio.cappella@roma1.infn.it (F.C.); antonella.incicchitti@roma1.infn.it (A.I.)
4 Dipartimento di Fisica, Università di Roma "La Sapienza", 00185 Rome, Italy
5 INFN, Laboratori Nazionali del Gran Sasso, Assergi, 67100 L'Aquila, Italy; matthias.laubenstein@lngs.infn.it (M.L.); stefano.nisi@lngs.infn.it (S.N.)
6 Arthur B. McDonald Canadian Astroparticle Physics Research Institute, Department of Physics, Engineering Physics and Astronomy, Queen's University, Kingston, ON K7L 3N6, Canada; serge.nagorny@lngs.infn.it (S.N.); wang.peng@queensu.ca (P.W.)
7 Department of Physics, Engineering Physics and Astronomy, Queen's University, Kingston, ON K7L 3N6, Canada
8 Department of Chemistry, Queen's University, Kingston, ON K7L 3N6, Canada
* Correspondence: vincenzo.caracciolo@roma2.infn.it

Simple Summary: Nuclear instability is an interesting topic which plays an important role in nuclear models, electroweak interaction e conservation laws. Herein, investigations on rare nuclear processes in Hf isotopes, using HP-Ge spectrometry and Hf-based crystal scintillators, are described. This type of investigation can be crucial in developing models in nuclear and astroparticle physics. In addition to the already-observed alpha decay of ^{174}Hf, some other rare nuclear processes, such as the alpha decay of ^{176}Hf in ^{172}Yb and ^{177}Hf in ^{173}Yb are near the theoretical expectations, giving hope to their first observation in the near future. In addition, a short emphasis on several types of Hf-based crystal scintillators is reported.

Abstract: In this work, a review of recent studies concerning rare nuclear processes in Hf isotopes is presented. In particular, the investigations using HP-Ge spectrometry and Hf-based crystal scintillators are focused; the potentiality and the results of the "source = detector" approach are underlined. In addition, a short introduction concerning the impact of such kind of research in the context of astroparticle and nuclear physics is pointed out. In particular, the study of α decay and double beta decay of ^{174}Hf, ^{176}Hf, ^{177}Hf, ^{178}Hf, ^{179}Hf, ^{180}Hf isotopes either to the ground state or to the lower bounded levels have been discussed. The observation of α decay of ^{174}Hf isotope to the ground state with a $T_{1/2} = 7.0(1.2) \times 10^{16}$ y is reported and discussed. No decay was detected for α decay of ^{174}Hf isotope at the first excited level of daughter and of ^{176}Hf, ^{177}Hf, ^{178}Hf, ^{179}Hf, ^{180}Hf isotopes either to the ground state or to the lower bounded levels. The $T_{1/2}$ lower limits for these decays are at the level of 10^{16}–10^{20} y. Nevertheless, the $T_{1/2}$ lower limits for the transitions of ^{176}Hf $\rightarrow$ ^{172}Yb ($0^+ \rightarrow 0^+$) and ^{177}Hf $\rightarrow$ ^{173}Yb ($7/2^- \rightarrow 5/2^-$) are near to the theoretical predictions, giving hope to their observation in the near future. All the other experimental limits ($\sim 10^{16}$–10^{20} y) are absolutely far from the theoretical expectations. The experiments investigating the 2ϵ and $\epsilon\beta^+$ processes in ^{174}Hf are also reported; the obtained half-life limits are set at the level of 10^{16}–10^{18} y. Moreover, we estimate the $T_{1/2}$ of $2\nu2\epsilon$ of ^{174}Hf decay at the level of (0.3–6) $\times 10^{21}$ y (at now the related measured lower limit is 7.1×10^{16} y).

Keywords: Hf; double beta decay; alpha decay; Cs_2HfCl_6

check for updates

Citation: Caracciolo, V.; Belli, P.; Bernabei, R.; Cappella, F.; Cerulli, R.; Incicchitti, A.; Laubenstein, M.; Leoncini, A.; Merlo, V.; Nagorny, S.; et al. Investigation on Rare Nuclear Processes in Hf Nuclides. *Radiation* **2022**, *2*, 234–247. https://doi.org/10.3390/radiation2020017

Academic Editor: Gabriele Multhoff

Received: 27 April 2022
Accepted: 26 May 2022
Published: 31 May 2022

Publisher's Note: MDPI stays neutral with regard to jurisdictional claims in published maps and institutional affiliations.

1. Introduction

A fascinating topic of nuclear physics is the nuclear instability, which plays an important role in nuclear models, electroweak interaction, and conservation laws. Here, the current status of the experimental searches for rare α and double beta decay (DBD) in Hf-isotopes is reviewed.

The DBD is a significant nuclear decay for neutrino physics, to test, e.g., the calculations of different nuclear shapes and the decay modes that involve the vector and axial-vector weak effective coupling constants (g_A), etc. The DBD with neutrinos is a higher-order effect with respect to the β-decay: the expected half-lives are longer than those of the β-decay, and roughly of the order of $\simeq 10^{20}$ y. Therefore, special experimental care has to be taken to study this process. The DBD without neutrinos emission is a process requiring lepton-number violation, in addition to a non-vanishing neutrino mass that requires a Majorana mass component. Therefore, it could be often regarded as the golden-standard process for probing the fundamental nature of neutrinos. Thus, the 0νDBD is of great interest because it could open a new window beyond the Standard Model. The number of candidate isotopes to this study are 69, in particular, 35 via the emission of two e^- and 34 in positive channels: either two positron emission ($2\beta^+$) or a positron emission with an electron capture ($\epsilon\beta^+$) or a double electron capture (2ϵ) [1,2]. The simultaneous study of positive and negative DBD can constrain the theoretical parameters with very high confidence, giving mutual information. Additionally, the nuclear matrix elements for the 2ν transition and 0ν transition can be connected through significant parameters: in the free nucleon interaction, the g_A value is 1.2701, but, considering a nuclear decay, the phenomenological axial-vector coupling value seams reduced to $g_A < 1$, more precisely: $g_A \sim 1.269A^{-0.12}$ or $g_A \sim 1.269A^{-0.18}$, depending on the adopted nuclear model [1]. Moreover, the "quenched" g_A observed is shown to encode the emergence of chiral-scale symmetry hidden in QCD in the vacuum; the g_A value could impact the in-medium modified nucleon weak and electromagnetic form factors on the neutrino mean free path in dense matter; the g_A role in the values of the cross sections of neutrino scattering from astrophysical sources on nuclei; and many other issues. Thus, DBD investigation considering different nuclei would help to constrain these and other significant model-dependent parameters. In addition, in case of the $0\nu 2\epsilon$ transition, it is possible to study also the so-called "resonant effect" [1,2].

Besides these, various nuclear models are continuously extended or improved, inspired, for example, by studying long-lived or stable superheavy isotopes and the predictions of their half-lives. Thus, the study of rare alpha decay plays a crucial role in developing nuclear physics. It can offer details about the nuclear structure, its levels and properties. Furthermore, the phenomenon of α decay can provide information about the fusion-fission reactions since the α decay process involves sub-barrier penetration due to the interaction between the nucleus and the α particle [3]. Moreover, understanding the nuclear properties is essential also for nuclear and particle astrophysics studies, for example, α–capture reactions (equivalent to the inverse α–decay process) are important for nucleosynthesis and β–delayed fission, together with other fission modes, determine the so-called "fission recycling" in the r-process nucleosynthesis [4]. In addition, as a byproduct, such researches contribute to develop new detectors and perform news protocols to purify materials containing DBD or rare α emitters from radio-impurities [5–25]. In this work, main aspects on status of the investigations on rare nuclear processes in Hf isotopes are reported.

2. Searching for Double Beta Decay in Hafnium Isotopes

The ^{174}Hf isotope is a potentially DBD emitter via $\epsilon\beta^+$ and 2ϵ modes with the energy decay $Q_{2\beta} = 1100.0(23)$ keV [26] and an isotopic abundance $\delta = 0.156(6)\%$ [27]. A simplified $\epsilon\beta^+$ and 2ϵ decay scheme of ^{174}Hf is shown in Figure 1. Theoretical half-life estimations of the $\epsilon\beta^+$ and 2ϵ of ^{174}Hf are not present in literature (to our knowledge) but the values of the phase space factor involved are (0.001–7.5) $\times$ 10^{-30} y^{-1} and (0.003–1) $\times$ 10^{-17} y^{-1} respectively for the $2\nu\epsilon\beta^+$ and $0\nu\epsilon\beta^+$ transitions [28] and

$(1.6 - 3.5) \times 10^{-21}$ y^{-1} for the $2\nu 2\epsilon$ transition [28]. Considering that typically the magnitude of the nuclear matrix element of the 2νDBD is of the order of 1–10, the half-life estimations are roughly 10^{28}–10^{33} y and (0.3–6) $\times$ 10^{21} y respectively for the $2\nu\epsilon\beta^+$ and $2\nu 2\epsilon$ transitions.

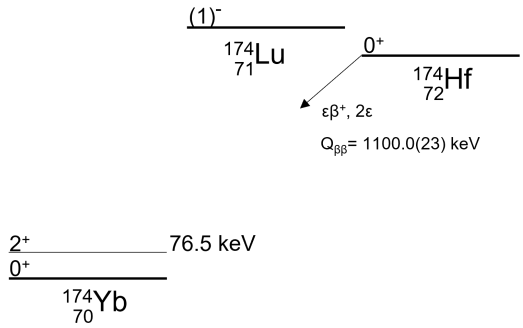

Figure 1. Simplified $\epsilon\beta^+$ and 2ϵ decay scheme of ^{174}Hf.

In 2020 and 2021 two independent experiments [29,30] (they are the first searches ever realized for 2ϵ and $\epsilon\beta^+$ decay of ^{174}Hf and for the work in Ref. [29] also by using a high-pure sample of hafnium), the first one performed at HADES laboratory of the Joint Research Centre of European Commission (Geel, Belgium) and the second one at the underground National Laboratory of Gran Sasso (LNGS) in Italy, searched for the 2ϵ and $\epsilon\beta^+$ decay of ^{174}Hf. In both cases, a passive approach (the source of the event searched for is outside the detector), using gamma-ray spectrometry technique, has been adopted. Both the experiments have adopted two different geometrical arrangements to increase the detection efficiency and to decrease as much as possible the energy threshold.

The experiment at HADES in Ref. [29] used a sample of metallic hafnium with sizes ⌀59.0 mm $\times$ 5.0 mm (total mass of 179.8 g that contained ∼0.29 g of the isotope ^{174}Hf). The experimental set-up was arranged using two different couples of HP-Ge detectors, and the Hf-sample was installed between the end-cap of two HP-Ge detectors arranged back-to-back (see Figure 2-left). The total exposure of the experiment was 42 g $\times$ d for the isotope ^{174}Hf.

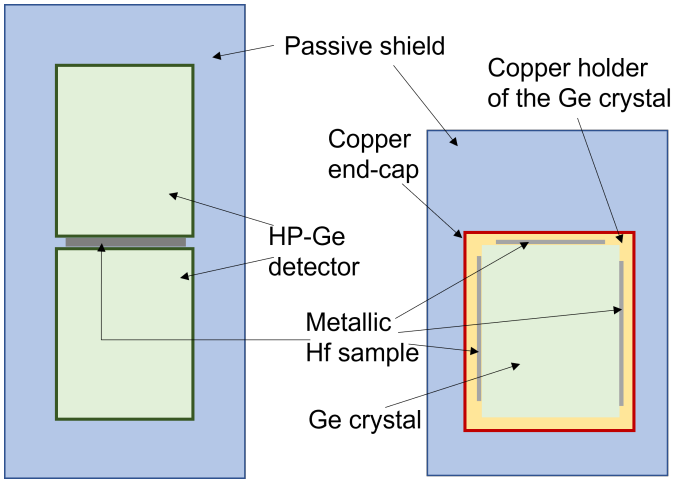

Figure 2. Simplified schematic representation of the experimental setups (not in scale) detailed in Refs. [29] (for the **left** scheme) and [30] (for the **right** scheme).

The experiment at LNGS on Ref. [30] used a foil of metallic hafnium of 55.379(1) g and the HP-Ge (⌀70 mm $\times$ 70 mm) was covered by this hafnium foil (see Figure 2-right). In particular, the foil thickness (0.25(1) mm) was optimized to minimize the self-absorption of low-energy γ and X-rays within the sample itself and improve the overall detection

efficiency; infact, the metallic foils were coupled to the Ge crystal (under its end-cap). The data were collected over 310 d.

The total exposures of those experiments were 26.9 kg × d and 16.5 kg × d for Ref. [29] and Ref. [30] respectively. In the Table 1 the detection efficiencies of both the experiments are compared (when possible); typically the experiment at Ref. [30] has higher values with respect to the other experiment.

Table 1. The detection efficiency of some 2ϵ and $\epsilon\beta^+$ processes in ^{174}Hf as performed in Refs. [29,30] if comparable. E_γ is the γ quanta used in both the experiments to study the half-life of the related transition.

Channel of the Decay	Decay Mode	Level of Daughter Nucleus J^π, Energy (keV)	E_γ (keV)	Detection Efficiency (%)	
				[29]	[30]
$2L$	2ν	2^+, 76.5	76.5	0.39	3.15
$2K$	0ν	g.s.	977.4	4.53	7.59
KL	0ν	g.s.	1028.9	4.46	7.32
$2L$	0ν	g.s.	1080.4	4.39	7.09
$2K$	0ν	2^+, 76.5	900.9	4.67	8.01
KL	0ν	2^+, 76.5	952.4	4.59	7.72
$2L$	0ν	2^+, 76.5	1003.9	4.51	7.45
$K\beta^+$	$2\nu + 0\nu$	g.s.	511	10.6	11.8
$L\beta^+$	$2\nu + 0\nu$	g.s.	511	10.7	11.8

Considering the 2ϵ transitions, in case of a $2K$ o KL capture in ^{174}Hf, a cascade of X-rays (and Auger electrons) of ^{174}Yb atom with energies in the range of (50.8–61.3) keV is expected, while energies of the $2L$ capture X-ray quanta are $\simeq$(7–10) keV. These latter were below the detectors' energy thresholds of both the experiments. Thank to these X-rays, the decay modes $2K$ and KL to the ground state (g.s.) of the ^{170}Yb have been studied by both experiments, besides the transition to the first excited level of the daughter nucleus. In both the investigations, the energy spectrum in the region of interest for the 2ν2K and 2νKL was dominated by the background due to the electron capture of ^{175}Hf ($T_{1/2}$ = 70(2) d; $Q_{EC} = 683.9(20)$ keV), but also from events related to U/Th chains, as clearly shown in the Figure 3a,b. In Refs. [29,30] no peculiarity have been observed concerning the DBD of ^{174}Hf; thus, in Table 2, the half-life limits are reported.

Table 2. The half-life limits of 2ϵ and $\epsilon\beta^+$ processes in ^{174}Hf as performed in Refs. [29,30].

Channel of the Decay	Decay Mode	Level of Daughter Nucleus J^π, Energy (keV)	Experimental Limit of $T_{1/2}$ (90% C.L. (y))	
			[29]	[30]
$2K$	2ν	g.s.	$\geq 7.1 \times 10^{16}$	$\geq 1.4 \times 10^{16}$
KL	2ν	g.s.	$\geq 4.2 \times 10^{16}$	$\geq 1.4 \times 10^{16}$
$2K$	2ν	2^+, 76.5	$\geq 5.9 \times 10^{16}$	$\geq 7.9 \times 10^{16}$
KL	2ν	2^+, 76.5	$\geq 3.5 \times 10^{16}$	$\geq 7.9 \times 10^{16}$
$2L$	2ν	2^+, 76.5	$\geq 3.9 \times 10^{16}$	$\geq 7.9 \times 10^{16}$
$2K$	0ν	g.s.	$\geq 5.8 \times 10^{17}$	$\geq 2.7 \times 10^{18}$
KL	0ν	g.s.	$\geq 1.9 \times 10^{18}$	$\geq 4.2 \times 10^{17}$
$2L$	0ν	g.s.	$\geq 7.8 \times 10^{17}$	$\geq 3.6 \times 10^{17}$
$2K$	0ν	2^+, 76.5	$\geq 7.1 \times 10^{17}$	$\geq 2.4 \times 10^{18}$
KL	0ν	2^+, 76.5	$\geq 6.2 \times 10^{17}$	$\geq 3.1 \times 10^{17}$
$2L$	0ν	2^+, 76.5	$\geq 7.2 \times 10^{17}$	$\geq 9.4 \times 10^{17}$
$K\beta^+$	$2\nu + 0\nu$	g.s.	$\geq 1.4 \times 10^{17}$	$\geq 5.6 \times 10^{16}$
$L\beta^+$	$2\nu + 0\nu$	g.s.	$\geq 1.4 \times 10^{17}$	$\geq 5.6 \times 10^{16}$

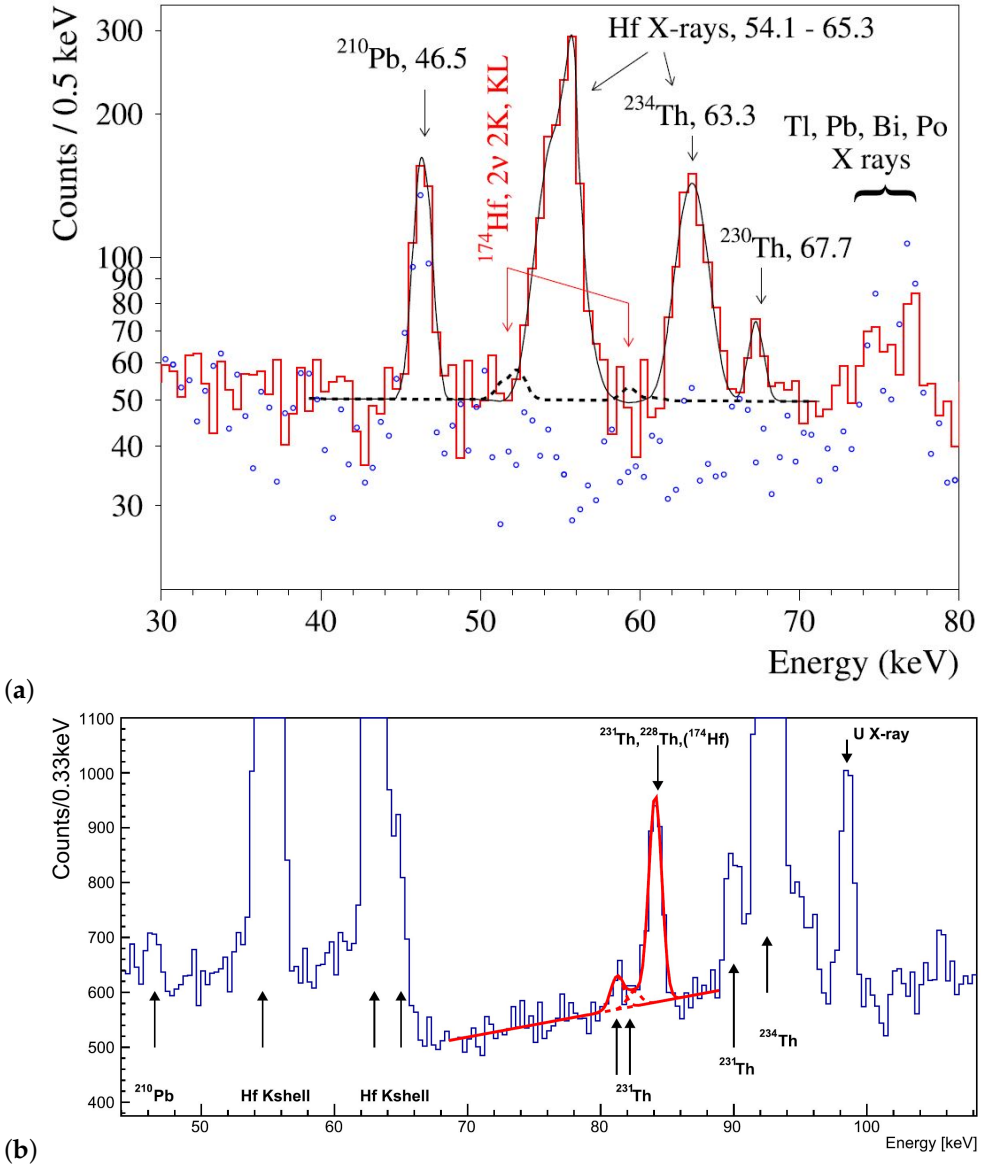

Figure 3. (**a**) Energy spectrum acquired with the experiment at HADES [29] in the region of interest for the $2\nu 2$K and 2νKL of ^{174}Hf (solid histogram, online red). The dots (online blue) is the background data without the Hf sample and normalized to the time of acquisition. Solid line (online black) is the fit of the background model, and the dashed line is the excluded effect. (Taken from Ref. [29] with permission). (**b**) Energy spectrum acquired with the experiment at LNGS [30], in the region of interest for the α decay of ^{174}Hf (see next section). However, the low energy range of the panel shows the energy region of interest for the case of $2\nu 2$K and 2νKL of ^{174}Hf decay, where the dominant background is due to the Hf X-rays. The solid line (online red) is the background model for the α decay of ^{174}Hf and the dashed line is the excluded effect. (Taken from Ref. [30] with permission).

3. Searching for Alpha Decays in Hafnium Isotopes

Natural hafnium consists of six isotopes: ^{174}Hf, ^{176}Hf, ^{177}Hf, ^{178}Hf, ^{179}Hf, ^{180}Hf; all of them are theoretically unstable concerning the α decay with a Q_α value in the range of 1.3–2.5 MeV. The Hf isotopes with natural abundance and with $Q_\alpha > 0$ are listed in the Table 3. All of them can decay to g.s. or to excited levels of daughter nuclei. Figure 4 shows simplified decay schemes of the α decay of the naturally occurring Hf isotopes.

Table 3. Main potential α decay of Hf nuclides. Isotopes with natural abundance (δ) greater than zero (i.e., naturally present in nature) and with $Q_\alpha > 0$ for transitions between g.s. or between g.s. and lowest bounded level (with spin/parity J^π) are listed. Theoretical predictions and experimental measurements (if exist) on the $T_{1/2}$'s are reported in the latest columns.

Nuclide Transition	J^π **Parent → Daughter Nuclei and Its Level (keV)**	δ (%) [31]	Q_α **(keV)** [26]	**$T_{1/2}$ (y)**			
				Experimental	**Theoretical**		
					[32]	[33]	[34]
^{174}Hf → ^{170}Yb	$0^+ \to 0^+$, g.s. $0^+ \to 2^+$, 84.2	0.156(6) [27]	2494.5(2.3)	$7.0(1.2) \times 10^{16}$ [27] $\geqslant 2.8 \times 10^{16}$ [30]	3.5×10^{16} 1.3×10^{18}	7.4×10^{16} 3.0×10^{18}	3.5×10^{16} 6.6×10^{17}
^{176}Hf → ^{172}Yb	$0^+ \to 0^+$, g.s. $0^+ \to 2^+$, 78.7	5.26(70)	2254.2(1.5)	$\geqslant 9.3 \times 10^{19}$ [27] $\geqslant 3.0 \times 10^{17}$ [35]	2.5×10^{20} 1.3×10^{22}	6.6×10^{20} 3.5×10^{22}	2.0×10^{20} 4.9×10^{21}
^{177}Hf → ^{173}Yb	$7/2^- \to 5/2^-$, g.s. $7/2^- \to 7/2^-$, 78.6	18.60(16)	2245.7(1.4)	$\geqslant 3.2 \times 10^{20}$ [27] $\geqslant 1.3 \times 10^{18}$ [35]	4.5×10^{20} 9.1×10^{21}	5.2×10^{22} 1.2×10^{24}	4.4×10^{22} 3.6×10^{23}
^{178}Hf → ^{174}Yb	$0^+ \to 0^+$, g.s. $0^+ \to 2^+$, 76.5	27.28(28)	2084.4(1.4)	$\geqslant 5.8 \times 10^{19}$ [27] $\geqslant 1.3 \times 10^{18}$ [30]	3.4×10^{23} 2.4×10^{25}	1.1×10^{24} 8.1×10^{25}	2.2×10^{23} 7.1×10^{24}
^{179}Hf → ^{175}Yb	$9/2^+ \to 7/2^+$, g.s. $9/2^+ \to 9/2^+$, 104.5	13.62(11)	1807.7(1.4)	$\geqslant 2.5 \times 10^{20}$ [27] $\geqslant 2.7 \times 10^{18}$ [30]	4.5×10^{29} 2.0×10^{32}	4.0×10^{32} 2.5×10^{35}	4.7×10^{31} 2.2×10^{34}
^{180}Hf → ^{176}Yb	$0^+ \to 0^+$, g.s. $0^+ \to 2^+$, 82.1	35.08(33)	1287.1(1.4)	– $\geqslant 1.0 \times 10^{18}$ [35]	6.4×10^{45} 4.0×10^{49}	5.7×10^{46} 4.1×10^{50}	9.2×10^{44} 2.1×10^{48}

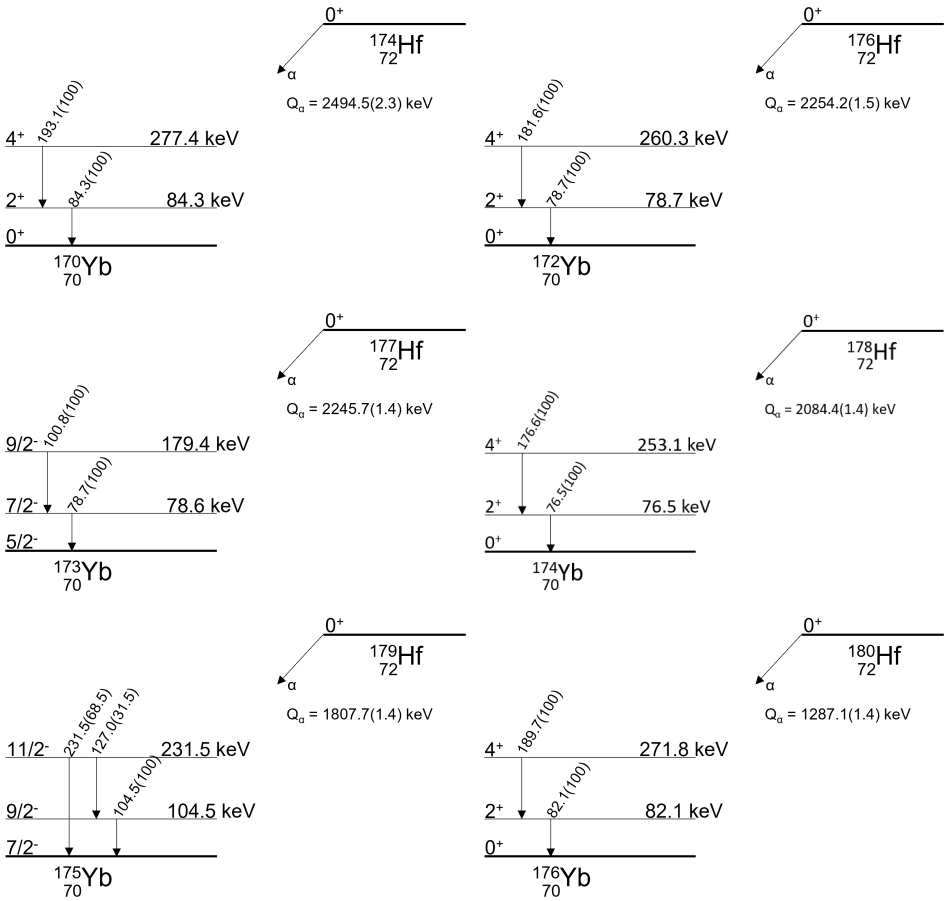

Figure 4. Simplified decay schemes of potential α decay of Hf isotopes considering the first two energy levels of the daughter nuclei. The corresponding gamma transitions and the probability related for a single energy level are also shown. The ^{175}Yb isotope is unstable via β^- decay with $T_{1/2} = 4.185(1)$ d [36], all the other Yb nuclei are stable.

In the decays of such Hf isotopes to excited levels, γ quanta are emitted. In this case, a search by using low-background γ spectrometry can be implemented. Moreover, because the ^{175}Yb is unstable via β^- decay with $T_{1/2} = 4.185(1)$ d [36], the ^{179}Hf to the g.s. of daughter ^{175}Yb can be evaluated using the mentioned passive technique.

Besides, the nuclide ^{178m2}Hf, the excited state of ^{178}Hf with energy 2446.1 keV, has a long half-life $T_{1/2} = 31(1)$ y [37]. Ordinarily, its de-excitation happens through $^{178m2}\text{Hf} \longrightarrow {}^{178}\text{Hf}$ transition. However, the α decay of $^{178m2}\text{Hf} \longrightarrow {}^{174}\text{Yb}$ is energetically possible with $Q_\alpha = 4530$ keV. In addition, the β^- decay to ^{178}Ta ($Q_{\beta^-} = 606$ keV), the electron capture to ^{178}Lu ($Q_\epsilon = 349$ keV) and the spontaneous fission ($Q_{SF} \simeq 100$ MeV) are also possible [38].

Considering that approach and using HP-Ge detectors, two experimental set-ups were realized (see Refs. [30,35]). Such setups are the same as those described in Section 2; they are the first experiments performed to study the α decay of ^{176}Hf, ^{177}Hf, ^{178}Hf, ^{179}Hf and ^{180}Hf, but considering only the transitions emitting gamma quanta. Thus, in Refs. [30,35], the decays, at the first excited level of the daughter nucleus, have been studied, as well as the ^{179}Hf to the g.s. of the daughter ^{175}Yb, thanks to its β^- instability (see Figure 4). The α decay of ^{174}Hf to the g.s. of ^{170}Yb was studied for the first time in Ref. [39]. In that case, a large cylindrical ionization counter has been used for measurements of natural alpha radioactivity. The heavy element samples were deposited uniformly over the internal surface of the cylindrical chamber, directly on the copper or the steel of the chamber (total active surface of 1200 cm^2). The gas mixture used was 94% argon, 5% ethylene, and 1% nitrogen. The measurements on the Hf sample were performed in two stages. In the first one a sample of HfO_2 enriched in ^{174}Hf was deposited with an average thickness of

0.10 mg $\times$ cm^{-2} and a weak ^{210}Po standard was added. A small peak was observed at 2.50 MeV. In the second stage, the HfO_2 sample was mixed with a small amount of Sm_2O_3, to try to improve the energy calibration of the data considering the peak position of ^{147}Sm, claiming that the $T_{1/2} = (4.0 \pm 0.2) \times 10^{15}$ y. However, the theoretical expectation (see Table 3) was in strong tension with the observation claimed.

Recently, an interesting experiment, using an active approach, was performed in Ref. [27] to study some potentially α decay of Hf isotopes to g.s. or exited levels of daughter nuclei and in particular the α decay of ^{174}Hf to the g.s. of ^{170}Yb. The best obtained results are reported in Table 3 with the theoretical estimations. In particular, Ref. [27] reports a direct study of the α decay of naturally occurring Hf isotopes by exploiting the "source = detector" approach with a Cs_2HfCl_6 (CHC) crystal scintillator. There, after 2848 h of data taking, the α decay of ^{174}Hf was observed with $T_{1/2} = 7.0(1.2) \times 10^{16}$ y. The experiment was carried out at the STELLA facility of the LNGS. The CHC crystal scintillator with mass 6.90(1) g was coupled with a 3-inch low radioactivity photomultiplier (PMT, Hamamatsu R6233MOD), and placed above the end-cap of the ultra-low background HP-Ge γ spectrometer GeCris (465 cm^3). A schematic cross-sectional view of the experimental set-up is shown in Ref. [27].

The crystal surface was wrapped by diffusive Polytetrafluoroethylene (PTFE) tape to enhance the light collection. The CHC and HP-Ge detectors were installed inside a passive shield, all in a plexiglas box continuously flushed by high purity nitrogen gas.

A CAEN DT5720B digitizer, as an event-by-event system, acquired the pulse profiles from the PMT and HP-Ge. In this way, it was possible to implement a coincidence logic between the events in the CHC and HP-Ge to study the α decay of Hf isotopes to the first excited level of the daughter nucleus when a γ–ray of such a decay is emitted and can reach the HP-Ge detector.

The pulse-shape discrimination (PSD) between β/γ and α particles, the time–amplitude analysis of fast correlated α decays, and the so-called Bi–Po events analysis were adopted to estimate the radioactive contamination of the CHC crystal. In particular, to build the background model, the data of the radioactive contamination of the CHC crystal was considered.

The time shape of each event was utilised to determine its "mean time" ($\langle t \rangle$) according to:

$$\langle t \rangle = \sum f(t_k) t_k / \sum f(t_k) \quad (1)$$

where the sum is over the time channels, k, starting from the origin of the pulse up to 8 µs. Moreover, $f(t)$ is the digitized amplitude (at the time t) of a given signal. Figure 5 shows the scatter plot of the $\langle t \rangle$ versus the energy for the acquired data. It confirms the good pulse-shape discrimination ability of the CHC detector [40]. The distribution of the $\langle t \rangle$ for the events with energies—using the γ scale—in the interval (0.4–3.0) MeV is reported in the inset of Figure 5. In Figure 6, the spectrum of α events according to the PSD analysis is given.

The Q.F.'s of the α particles at the energies of ^{224}Ra, ^{220}Rn and ^{216}Po α decays were measured to be 0.39(4), 0.40(3), 0.40(3), respectively, and shown in Figure 7 of Ref. [27] with the fit following the prescription of Ref. [41].

The α energy spectrum, above 4 MeV, was fitted (see Figure 6) using a model which includes the α peaks (see Ref. [27] for details) of ^{232}Th, ^{238}U and their daughters in order to study such contaminants (taking in account the measured Q.F.'s of the α particles). Considering all the α events, the total internal α activity in the CHC crystal is at the level of 7.8(3) mBq/kg. However, adopting the declared $T_{1/2}$ of the ^{174}Hf α decay in Ref. [39] (see before), the event numbers in 2848 h of data taking with this CHC crystal (see Ref. [27] for details) would be ~1100 counts. Nevertheless, all the measured α events was 553(23), even ascribing all of them to ^{174}Hf α decay (although considering the information reported above); thus, the result given in Ref. [39] is safely refused; in fact, even in such an unlike hypothesis, the $T_{1/2}$ value derived in Ref. [27] would be $4.01(17) \times 10^{15}$ y, about 4.5σ far from $T_{1/2} = 2.0(4) \times 10^{15}$ in Ref. [39]. Therefore, the half-life given in Ref. [39] was safely

rejected. Let us now report the improved determination of the half-life of the ^{174}Hf α decay thanks to the analysis in Ref. [27].

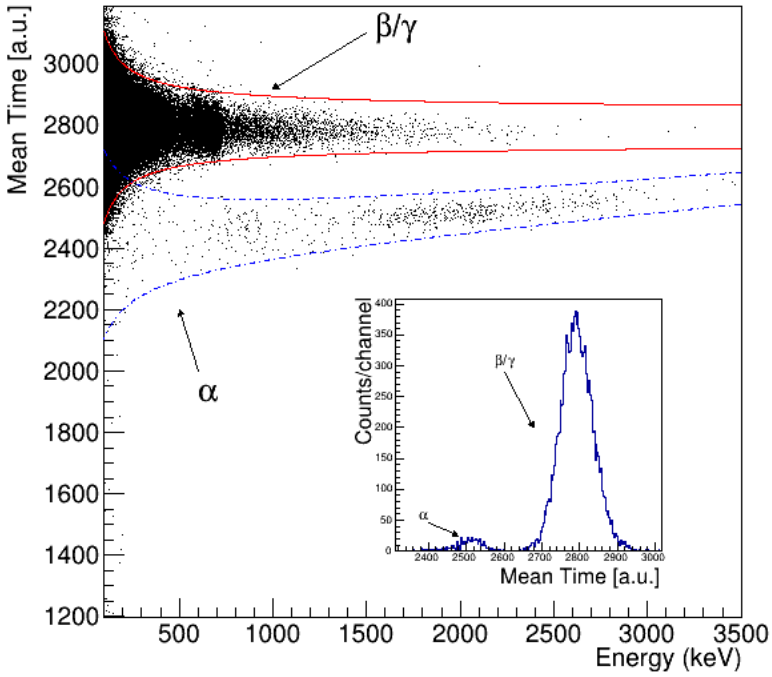

Figure 5. Mean time ($\langle t \rangle$) versus energy for the data accumulated over 2848 h using a CHC crystal scintillator (see text). The lines corresponding to sigma intervals (at the 99% of events) for the $\langle t \rangle$ values of β/γ and α particles are painted (on-line: red solid lines and blue dashed lines, respectively). (Inset) Distribution of the $\langle t \rangle$ for the data in the energy range of (0.4–3.0) MeV (taken from Ref. [27] with permission).

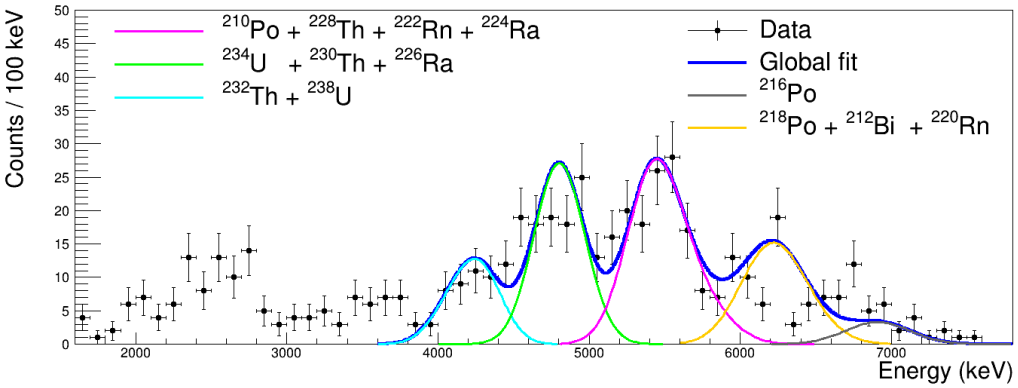

Figure 6. α energy spectrum picked out using the PSD from the data accumulated with the CHC crystal scintillator over 2848 h. The fit model built from α decays of ^{238}U and ^{232}Th with daughters is highlighted by blue solid line, and some individual fit contributions are also presented. The energy scale is in α energy having considered the Q.F. studied in Ref. [27] (taken from Ref. [27] with permission).

The background model in the range (1.1–3.9) MeV, where the ^{174}Hf α decay is expected too, was made by an exponential function (to take into account the residual β/γ events), some degraded alpha particles and suitable asymmetric Gaussian to shaping the α decay of ^{174}Hf ($Q_\alpha = 2494.5(2.3)$ keV), ^{147}Sm ($Q_\alpha = 2311.2(10)$ keV) and the data in the energy interval (3.0–3.9) MeV (see Ref. [27] for details). The fit, in the range (1.1–3.9) MeV, gives a $\chi^2/n.d.f. = 0.87$ (χ^2 probability = 38.7%) and 31.7(5.6) events for the signal searched for (see Figure 7-left).The peak near 2.3 MeV is ascribed to the α decay of ^{147}Sm and the

estimated number of counts is 29.5(5.4) in very good agreement with that expected for ^{147}Sm reported in Table 7 of Ref. [27]: 36(6) counts. The statistical impact of the other eligible radionuclides is negligible, as demonstrated in Ref. [27]. The Q_α values of ^{147}Sm and ^{174}Hf determined by the fit procedure show a slight shift in the same direction of the mean value (∼5%) consistent with the uncertainty of the adopted Q.F. model discussed in Ref. [27].

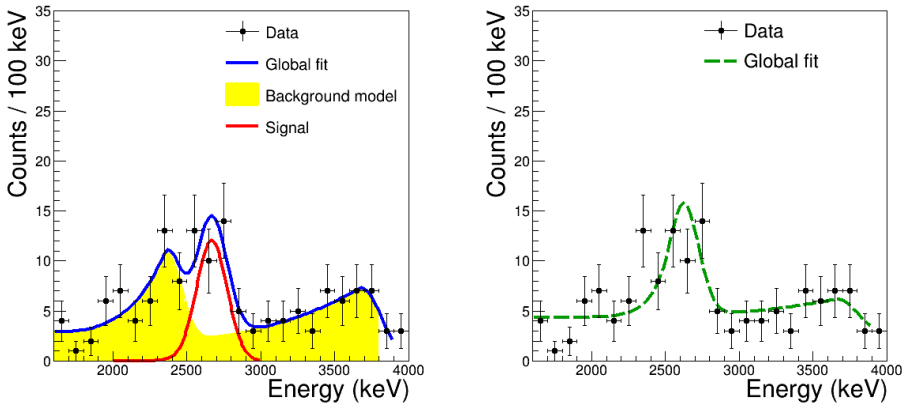

Figure 7. Using the PSD, the energy spectrum of α events from the acquired data with a CHC scintillator over 2848 h is shown. For the energy scale, the authors have considered the Q.F. of α particles (see text or Ref. [27] for details). (**left**) The fit of the data, in the energy region of interest, for the ^{174}Hf α decay. The fit model is built considering the α decays of ^{147}Sm, ^{174}Hf (red line) and taking into account some degraded alpha particles (online solid blue line). The yellow band is the background model. (**right**) The fit of the data by a modified model similar to the previous one but considering one peak (instead of two) in the energy (2.2–2.6) MeV (taken from Ref. [27] with permission).

To exclude that the data in the range (2–3) MeV could be due to one single peak, the previous fit was performed considering one single peak (see Figure 7-right). The fit result gives a *p*-value of 1.7%.

Thus, according to all the detailed analysis in Ref. [27] (2848 h of data taking with a CHC crystal of 6.09(1) g), the half-life for the ^{174}Hf α decay, is:

$$T_{1/2} = (7.0 \pm 1.2) \times 10^{16} \text{ y}. \quad (2)$$

4. Perspectives and Conclusions

In this work, the experimental studies and few $T_{1/2}$ predictions concerning the rare decay of naturally occurring isotopes have been briefly reported. In particular, in Table 2 the half-life limits of 2ϵ and $\epsilon\beta^+$ processes in ^{174}Hf are shown. The half-life limits are at the level of 10^{16}–10^{18} y. These values have to be compared to the values of the phase space factor predicted for such transition considering a nuclear matrix element of the order of 1–10 as typical for that calculations (see Section 2). In this case, it is interest to notice, that the $2\nu2\epsilon$ of ^{174}Hf decay has a $T_{1/2}$ estimation of (0.3–6) $\times 10^{21}$ y (at now the related measured lower limit is 7.1×10^{16} y). This encourages progress in such research, especially using the "detector = source" approach to profit a better detection efficiency with respect to the passive one.

In Table 3 the main potential α transition of Hf isotopes and the related experimental measurements and theoretical predictions of half-lives are reported. In particular, an experiment to investigate the α decay of naturally occurring hafnium isotopes to the first excited state and the ground state using a CHC crystal scintillator in coincidence with a HP-Ge detector was completed after 2848 h of live time (see Ref. [27]). The analysis performed ruled out the $T_{1/2}$ value of α decay of ^{174}Hf isotope given in Ref. [39]. Furthermore, Ref. [27] stated that the α decay of ^{174}Hf isotope to the ground state was observed with a

$T_{1/2} = 7.0(1.2) \times 10^{16}$ y. This value is in good agreement with the theoretical predictions reported in Table 3.

Besides this result, no decay was detected for α and DBD of ^{174}Hf, ^{176}Hf, ^{177}Hf, ^{178}Hf, ^{179}Hf, ^{180}Hf isotopes either to the ground state or to the lower bounded levels considering the data in Ref. [27,30,35]. The determined $T_{1/2}$ lower limits for these decays are reported in Table 3. In particular, the $T_{1/2}$ lower limits for the transitions of ^{176}Hf $\rightarrow$ ^{172}Yb ($0^+ \rightarrow 0^+$) and ^{177}Hf $\rightarrow$ ^{173}Yb ($7/2^- \rightarrow 5/2^-$) are near to the theoretical predictions (see Table 3); all the other limits ($\sim 10^{16}$–10^{20} y) are absolutely far from the theoretical expectations.

In Ref. [27], it has also been evaluated the average quenching factor for alpha particles modelled according to the prescription of Ref. [41] and reported in Figure 7 of Ref. [27]; it varies in the range 0.3–0.4. In addition, the CHC crystal scintillator of Ref. [27] exhibits a powerful PSD between β/γ and α events as proved in Figure 5.

For the future, the development and the use of scintillation detectors, containing the isotope of interest (as a "source= detector" approach), are a very reasonable way to improve the experimental sensitivity. One of the more promising scintillator is the mentioned Cs_2HfCl_6. In particular, such detector meets high detection efficiency, good particle discrimination capability, large amount of the isotope of interest, dedicated protocol of material selection and growing procedure, a low background, and a good energy resolution. Indeed, nowadays there is significant interest in the development of scintillating crystals from the metal hexachlorides Cs_2MCl_6 (M = Hf or other nuclei) family thanks to their outstanding scintillating properties—a high light yield (up to 50,000 photons/MeV), perfect linearity of the energy response, excellent energy resolution (<3.5% at 662 keV in the best configuration), a quenching factor for alpha particles around QF = 0.3–0.5, and excellent statistical pulse shape discrimination ability. For example, in Figure 8 we show the diagram $T_{1/2}$ vs the inverse of the square root of alpha energy in MeV. The black symbols are the results in Ref. [27]. The blue band is the extrapolation of the predictions on $T_{1/2}$ for all the Hf isotopes using the Geiger-Nuttall scaling law considering the data point observed in Ref. [27]. The red symbols represent the sensitivity that the measurement can reach using a CHC crystal scintillator with 43.83 kg $\times$ day of exposure. As evident, there is a good perspective to observe the α decay of ^{176}Hf and ^{176}Hf (see also Table 3). In addition, to further increase the sensitivity for the study of the rare α and 2β decays of naturally occurred hafnium isotopes with the active source approach, it is also relevant to improve the radiopurity of Cs_2HfCl_6 crystal scintillators, in particular for what concerns the Sm component in traces.

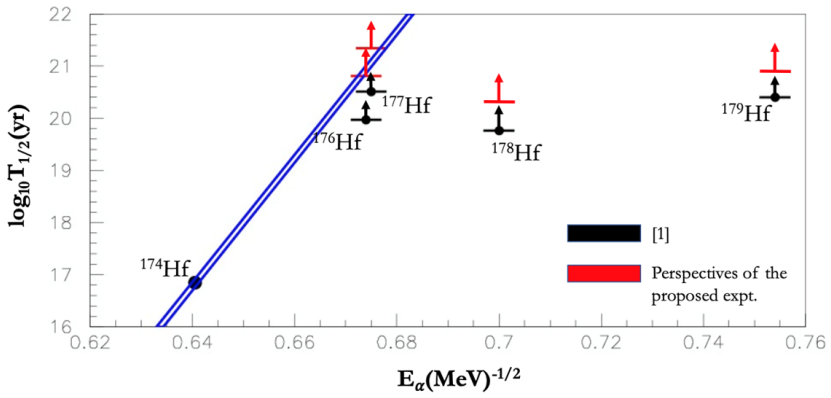

Figure 8. Diagram $T_{1/2}$ vs the inverse of the square root of alpha energy in MeV. The black symbols are the results in Refs. [1,27]. The α decay of ^{174}Hf has been observed [27], while only lower limits at 90% C.L. are reported for the other three Hf isotopes naturally present. The blue band is the extrapolation of the predictions for all the Hf isotopes using the Geiger-Nuttall scaling law and the observed data point [27]. The red symbols represent the sensitivity that the measurement can reach using a CHC crystal scintillator with 43.83 kg $\times$ day of exposure. As evident, there is a good perspective to observe the α decay of ^{176}Hf and ^{176}Hf (see also Table 3).

Besides this, some potential crystal scintillator containing Hf isotopes are the transparent optical ceramics based on cerium doped alkaline earth hafnates: $BaHfO_3$(Ce) and $SrHfO_3$(Ce) [42]; but also crystal scintillators as $CaHfO_3$ [43], HfF_4 [44], HfO_2 [45], $La_2Hf_2O_7$(Ti) [46], Tl_2HfCl_6 [47,48]. The main scintillation properties of such crystals are listed in Table 4. In general, an other promising approach is also a crystal that can work as scintillating bolometers to study the decays to the ground state of daughter nuclei [49]. HP-Ge, instead, is a promising choice for the investigations of decay to excited levels of daughter nuclei thanks the excellent energy resolution. Finally, an important issue is to use a crystal scintillator with high percentage in weight of Hf isotopes (see Table 4) or the implementation of isotopically enriched materials in the isotope of interest. However, in the our knowledge, no suitable technology existed that could guarantee a high concentration of a specific hafnium isotope, and the expensive enrichment process is mainly achieved by using the electromagnetic separation method.

Table 4. Main properties of Hf-based crystal scintillators (See text).

Scintillator	Percentage of Hf in Weight (%)	Density (g/cm^3)	L.Y. (phe/MeV)	Main Decay Time (ns)	Main Emission Peak (nm)
$BaHfO_3$(Ce)	49	8.3	∼40,000	∼25	∼400
$CaHfO_3$	67	6.9	∼10,000	∼33	∼439
Cs_2HfCl_6	31	3.8	∼50,000	∼10,000	∼400
HfF_4	70	7.1	∼300	∼29	∼350
HfO_2	85	9.7	∼30,000	∼9500	∼480
$La_2Hf_2O_7$(Ti)	23	7.9	∼13,000	∼10,000	∼475
$SrHfO_3$(Ce)	57	6.7	∼40,000	∼42	∼410
Tl_2HfCl_6	22	5.3	∼25,000	∼36 (89%); ∼217 (6%); ∼1500 (11%)	∼380

Author Contributions: All the authors of this paper have been significantly contributing to the presented review of experimental results. All authors have read and agreed to the published version of the manuscript.

Funding: This research received no external funding.

Institutional Review Board Statement: Not applicable.

Informed Consent Statement: Not applicable.

Data Availability Statement: Not applicable.

Conflicts of Interest: The authors declare no conflict of interest.

References

1. Belli, P.; Bernabei, R.; Caracciolo, V. Status and Perspectives of 2ϵ, $\epsilon\beta^+$ and $2\beta^+$ Decays. *Particles* **2021**, *4*, 241–274. [CrossRef]
2. Belli, P.; Bernabei, R.; Cappella, F.; Caracciolo, V.; Cerulli, R.; Incicchitti, A.; Merlo, V. Double Beta Decay to Excited States of Daughter Nuclei. *Universe* **2020**, *6*, 239. [CrossRef]
3. Belli, P.; Bernabei, R.; Danevich, F.A.; Incicchitti, A.; Tretyak, V.I. Experimental searches for rare alpha and beta decays. *Eur. Phys. J. A* **2019**, *55*, 140. [CrossRef]
4. Van Duppen, P.; Andreyev, A.N. Alpha Decay and Beta-Delayed Fission: Tools for Nuclear Physics Studies. The Euroschool on Exotic Beams. *Lect. Notes Phys.* **2018**, *948*, 65–116.
5. Belli, P.; Bernabei, R.; Cappella, F.; Caracciolo, V.; Cerulli, R.; Danevich, F.A.; Di Marco, A.; Incicchitti, A.; Poda, D.V.; Polischuk, O.G.; et al. Investigation of rare nuclear decays with BaF_2 crystal scintillator contaminated by radium. *Eur. Phys. J. A* **2014**, *50*, 134. [CrossRef]
6. Barabash, A.S.; Belli, P.; Bernabei, R.; Borovlev, Y.A.; Cappella, F.; Caracciolo, V.; Cerulli, R.; Danevich, F.A.; Incicchitti, A.; Kobychev, V.V.; et al. Improvement of radiopurity level of enriched $^{116}CdWO_4$ and $ZnWO_4$ crystal scintillators by recrystallization. *Nucl. Instrum. Meth. A* **2016**, *833*, 77–81. [CrossRef]

7. Danevich, F.A.; Barabash, A.S.; Belli, P.; Bernabei, R.; Boiko, R.S.; Brudanin, V.B.; Cappella, F.; Caracciolo, V.; Cerulli, R.; Incicchitti, A.; et al. Development of radiopure cadmium tungstate crystal scintillators from enriched ^{106}Cd and ^{116}Cd to search for double beta decay. *AIP Conf. Proc.* **2013**, *1549*, 201–204.
8. Belli, P.; Bernabei, R.; Brudanin, V.B.; Cappella, F.; Caracciolo, V.; Cerulli, R.; Danevich, F.A.; Incicchitti, A.; Kasperovich, D.V.; Klavdiienko, V.R.; et al. Search for Double Beta Decay of ^{106}Cd with an Enriched $^{106}CdWO_4$ Crystal Scintillator in Coincidence with $CdWO_4$ Scintillation Counters. *Universe* **2020**, *6*, 182. [CrossRef]
9. Leoncini, A.; Belli, P.; Bernabei, R.; Cappella, F.; Caracciolo, V.; Cerulli, R.; Danevich, F.A.; Incicchitti, A.; Kasperovich, D.V.; Klavdiienko, V.; et al. New results on search for 2β decay processes in ^{106}Cd using $^{106}CdWO_4$ scintillator. *Phys. Scr.* **2022**, *97*, 064006. [CrossRef]
10. Belli, P.; Bernabei, R.; Borovlev, Y.A.; Cappella, F.; Caracciolo, V.; Cerulli, R.; Danevich, F.A.; Degoda, V.Y.; Incicchitti, A.; Kasperovych, D.V.; et al. Optical, luminescence, and scintillation properties of advanced $ZnWO_4$ crystal scintillators. *Nucl. Instrum. Meth. A* **2022**, *1029*, 166400. [CrossRef]
11. Barabash, A.S.; Belli, P.; Bernabei, R.; Cappella, F.; Caracciolo, V.; Cerulli, R.; Chernyak, D.M.; Danevich, F.A.; d'Angelo, S.; Incicchitti, A.; et al. Final results of the Aurora experiment to study 2β decay of ^{116}Cd with enriched $^{116}CdWO_4$ crystal scintillators. *Phys. Rev. D* **2018**, *98*, 092007. [CrossRef]
12. Belli, P.; Bernabei, R.; Boiko, R.S.; Brudanin, V.B.; Cappella, F.; Caracciolo, V.; Cerulli, R.; Chernyak, D.M.; Danevich, F.A.; d'Angelo, S.; et al. Search for double-β decay processes in ^{106}Cd with the help of $^{106}CdWO_4$ crystal scintillator. *Phys. Rev. C* **2012**, *85*, 044610. [CrossRef]
13. Belli, P.; Bernabei, R.; Borovlev, Y.A.; Cappella, F.; Caracciolo, V.; Cerulli, R.; Danevich, F.A.; Incicchitti, A.; Kasperovych, D.V.; Polischuk, O.G.; et al. New development of radiopure $ZnWO_4$ crystal scintillators. *Nucl. Instrum. Meth. A* **2019**, *935*, 89–94. [CrossRef]
14. Bernabei, R.; Belli, P.; Cappella, F.; Caracciolo, V.; Castellano, S.; Cerulli, R.; Boiko, R.S.; Chernyak, D.M.; Danevich, F.A.; Incicchitti, A.; et al. Crystal scintillators for low background measurements. *AIP Conf. Proc.* **2013**, *1549*, 189–196.
15. Barucci, M.; Beeman, J.W.; Caracciolo, V.; Pagnanini, L.; Pattavina, L.; Pessina, G.; Pirro, S.; Rusconi, C.; Schäffnerfc, K. Cryogenic light detectors with enhanced performance for rare event physics. *Nucl. Instrum. Meth. A* **2019**, *935*, 150–155. [CrossRef]
16. Belli, P.; Bernabei, R.; Boiko, R.S.; Cappella, F.; Caracciolo, V.; Cerulli, R.; Chernyak, D.M.; Danevich, F.A.; di Vacri, M.L.; Incicchitti, A.; et al. First search for 2ϵ and $\epsilon\beta^+$ processes in ^{168}Yb. *Nucl. Phys. A* **2019**, *990*, 64–78. [CrossRef]
17. Barabash, A.S.; Belli, P.; Bernabei, R.; Boiko, R.S.; Cappella, F.; Caracciolo, V.; Cerulli, R.; Danevich, F.A.; Di Marco, A.; Incicchitti, A.; et al. Double beta decay of ^{150}Nd to the first excited 0^+ level of ^{150}Sm: Preliminary results. *Nucl. Phys. Atom. Energy* **2018**, *19*, 95–102. [CrossRef]
18. Belli, P.; Bernabei, R.; Boiko, R.S.; Cappella, F.; Caracciolo, V.; Cerulli, R.; Danevich, F.A.; Incicchitti, A.; Kropivyansky, B.N.; Laubenstein, M.; et al. First search for 2ϵ and $\epsilon\beta^+$ decay of ^{162}Er and new limit on 2β^- decay of ^{170}Er to the first excited level of ^{170}Yb. *J. Phys. G* **2018**, *45*, 095101. [CrossRef]
19. Barabash, A.S.; Belli, P.; Bernabei, R.; Cappella, F.; Caracciolo, V.; Cerulli, R.; Danevich, F.A.; Di Marco, A.; Incicchitti, A.; Kasperovych, D.V.; et al. Low background scintillators to investigate rare processes. *J. Instrum.* **2020**, *15*, C07037. [CrossRef]
20. Belli, P.; Bernabei, R.; Boiko, R.S.; Cappella, F.; Caracciolo, V.; Cerulli, R.; Danevich, F.A.; Di Marco, A.; Incicchitti, A.; Kropivyansky, B.N.; et al. First direct search for 2ϵ and $\epsilon\beta^+$ decay of ^{144}Sm and 2β^- decay of ^{154}Sm. *Eur. Phys. J. A* **2019**, *55*, 201. [CrossRef]
21. Belli, P.; Bernabei, R.; Cappella, F.; Caracciolo, V.; Cerulli, R.; Danevich, F.A.; Incicchitti, A.; Kasperovych, D.V.; Kobychev, V.; Kovtun, G.P.; et al. Search for α decay of naturally occurring osmium nuclides accompanied by γ quanta. *Phys. Rev. C* **2020**, *102*, 024605. [CrossRef]
22. Caracciolo, V.; Cappella, F.; Cerulli, R.; Di Marco, A.; Laubenstein, M.; Nagorny, S.S.; Safonova, O.E.; Shlegelh, N.G. Limits and performances of a $BaWO_4$ single crystal. *Nucl. Instrum. Meth. A* **2019**, *901*, 150–155. [CrossRef]
23. Azzolin, O.; Beeman, J.W.; Bellini, F.; Beretta, M.; Biassoni, M.; Brofferio, C.; Bucci, C.; Capelli, S.; Cardani, L.; Carniti, P.; et al. Measurement of ^{216}Po half-life with the CUPID-0 experiment. *Phys. Lett. B* **2021**, *822*, 136642. [CrossRef]
24. Belli, P.; Bernabei, R.; Boiko, R.S.; Danevich, F.A.; Di Marco, A.; Incicchitti, A.; Kasperovych, D.V.; Cappella, F.; Caracciolo, V.; Kobychev, V.V.; et al. Half-life measurements of ^{212}Po with thorium-loaded liquid scintillator. *Nucl. Phys. Atom. Energy* **2018**, *19*, 220–226. [CrossRef]
25. Belli, P.; Bernabei, R.; Cappella, F.; Caracciolo, V.; Cerulli, R.; Danevich, F.A.; Incicchitti, A.; Kasperovych, D.V.; Kobychev, V.; Kovtun, G.P.; et al. New experimental limits on double-beta decay of osmium. *J. Phys. G* **2021**, *48*, 085104. [CrossRef]
26. Wang, M.; Huang, W.J.; Kondev, F.G.; Audi, G.; Naimi, S. The AME 2020 atomic mass evaluation (II). Tables, graphs and references. *Chin. Phys. C* **2021**, *41*, 030003. [CrossRef]
27. Caracciolo, V.; Nagorny, S.S.; Belli, P.; Bernabei, R.; Cappella, F.; Cerulli, R.; Inchicchitti, A.; Laubenstein, M.; Merlo, V.; Nisi, S.; et al. Search for α decay of naturally occurring Hf-nuclides using a Cs_2HfCl_6 scintillator. *Nucl. Phys. A* **2020**, *1002*, 121941. [CrossRef]
28. Mirea, M.; Pahomi, T.; Stoica, S. Values of the phase space factors involved in double beta decay. *Rom. Rep. Phys.* **2015**, *67*, 872–889.
29. Danevich, F.A.; Hult, M.; Kasperovych, D.V.; Kovtunc, G.P.; Kovtun, K.W.; Lutter, G.; Marissens, G.; Polischuk, O.G.; Stetsenko, S.P.; Tretyak, V.I. First search for 2ϵ and $\epsilon\beta^+$ decay of ^{174}Hf. *Nucl. Phys. A* **2020**, *996*, 121703. [CrossRef]

30. Broerman, B.; Laubenstein, M.; Nagorny, S.; Songac, N.; Vincent, A.C. A search for rare and induced nuclear decays in hafnium. *Nucl. Phys. A* **2021**, *1012*, 122212. [CrossRef]
31. Meija, J.; Coplen, T.B.; Berglund, M.; Brand, W.A.; De Bièvre, P.; Gröning, M.; Holden, N.E.; Irrgeher, J.; Loss, R.D.; Walczyk, T.; et al. Atomic weights of the elements 2013. *Pure Appl. Chem.* **2016**, *88*, 293. [CrossRef]
32. Buck, B.; Merchant, A.C.; Perez, S.M. Ground state to ground state alpha decays of heavy even-even nuclei. *Physica G* **1991**, *17*, 1223. [CrossRef]
33. Poenaru, D.N.; Ivascu, M. Estimation of the alpha decay half-lives. *J. Phys.* **1983**, *44*, 791. [CrossRef]
34. Denisov, V.Y.; Khudenko, A.A. α-decay half-lives: Empirical relations. *Rhys. Rev. C* **2015**, *92*, 014602. [CrossRef]
35. Danevich, F.A.; Hult, M.; Kasperovych, D.V.; Kovtunc, G.P.; Kovtun, K.W.; Lutter, G.; Marissens, G.; Polischuk, O.G.; Stetsenko, S.P.; Tretyak, V.I. First search for α decays of naturally occurring Hf nuclides with emission of γ quanta. *Eur. Phys. J. A* **2020**, *56*, 5. [CrossRef]
36. Abzouzi, A.; Antony, M.S.; Ndocko Ndongué, V.B. Precision measurements of the half-lives of nuclides. *J. Rad. Nucl. Chem. Lett.* **1998**, *135*, 1–7. [CrossRef]
37. Achterberg, E.; Capurro, O.A.; Marti, G.V. Nuclear Data Sheets for A = 178. *Nucl. Data Sheets* **2009**, *110*, 1473. [CrossRef]
38. Van Klinken, J.; Venema, V.Z.; Janssens, R.V.F.; Emery, G.T. K-forbidden decays in ^{178}Hf; M4 decay of an Yrast state. *Nucl. Phys. A* **1980**, *339*, 189. [CrossRef]
39. Macfarlane, R.D.; Kohman, T.P. Natural alpha radioactivity in medium-heavy elements. *Phys. Rev.* **1961**, *121*, 1758. [CrossRef]
40. Cardenas, C.; Burger, A.; Goodwin, B.; Groza, M.; Laubenstein, M.; Nagorny, S.; Rowe, E. Pulse-shape discrimination with Cs_2HfCl_6 crystal scintillator. *Nucl. Inst. Met. A* **2017**, *869*, 63–67. [CrossRef]
41. Tretyak, V.I. Semi-empirical calculation of quenching factors for ions in scintillators. *Astropart. Phys.* **2010**, *33*, 40. [CrossRef]
42. van Loef, E.V.; Higgins, W.M.; Glodo, J.; Brecher, C.; Lempicki, A.; Venkataramani, V.; Moses, W.W.; Derenzo, E.S.; Shah, K.S. Scintillation Properties of $SrHfO_3$(Ce) and $BaHfO_3$(Ce) Ceramics. *IEEE Trans. Nucl. Sci.* **2007**, *54*, 741–743. [CrossRef]
43. Derenzo, S.; Bizarri, G.; Borade, R.; Bourret-Courchesne, E.; Boutchko, R.; Canning, A.; Chaudhry, A.; Eagleman, Y.; Gundiah, G.; Hanrahan, S.; et al. New scintillators discovered by high-throughput screening. *Nucl. Instr. Meth. A* **2011**, *652*, 247–250. [CrossRef]
44. Derenzo, S.E.; Moses, W.W.; Cahoon, J.L.; Perera, R.C.C.; Litton, J.E. Prospects for New Inorganic Scintillators. *IEEE Trans. Nucl. Sci.* **1990**, *37*, 203–208. [CrossRef]
45. LeLuyer, C.; Villanueva-Ibanez, M.; Pillonnet, A.; Dujardin, C. HfO_2:X (X = Eu^{3+}, Ce^{3+}, Y^{3+}) Sol Gel Powders for Ultradense Scintillating Materials. *J. Phys. Chem. A* **2008**, *112*, 10152–10155. [CrossRef] [PubMed]
46. Ji, Y.M.; Jiang, D.Y.; Shi, J.L. $La_2Hf_2O_7$:Ti^{4+} ceramic scintillator for x-ray imaging. *J. Mater. Rese.* **2005**, *20*, 567–570. [CrossRef]
47. Fujimoto, Y.; Saeki, K.; Nakauchi, D.; Yanagida, T.; Koshimizu, M.; Asai, K. New Intrinsic Scintillator with Large Effective Atomic Number: Tl_2HfCl_6 and Tl_2ZrCl_6 Crystals for X-ray and Gamma-ray Detections. *Sens. Mater.* **2018**, *30*, 1577–1583. [CrossRef]
48. Vuong, P.Q.; Tyagi, M.; Kim, S.H.; Kim, H.J. Crystal growth of a novel and efficient Tl_2HfCl_6 scintillator with improved scintillation characteristics. *Cryst. Eng. Comm.* **2019**, *21*, 5898–5904. [CrossRef]
49. Dumoulin, L.; Giuliani, A.; Kandel, R.; Khalife, H.; Kuznetsov, S.V.; Nagorny, S.S.; Nahorna, V.V.; Nishchev, K.N.; Nones, C.; Olivieri, E.; et al. Assessment of Cs_2HfCl_6 crystal applicability as low-temperature scintillating bolometers by their thermodynamic characteristics. *J. Mater. Chem. C* **2022**, *10*, 5218–5229. [CrossRef]